

# A NOVEL MICROWAVE SENSOR WITH HIGH-Q SYMMETRICAL SPLIT RING RESONATOR FOR MATERIAL PROPERTIES MEASUREMENT

Rammah A. Alahnomi<sup>a</sup>, Z. Zakaria<sup>a\*</sup>, E. Ruslan<sup>b</sup>, Amyrul Azuan Mohd Bahar<sup>a</sup>, Noor Azwan Shairi<sup>a</sup>

<sup>a</sup>Centre for Telecommunication Research and Innovation (CeTRI), Universiti Teknikal Malaysia Melaka (UTeM), 76100 Durian Tunggal, Melaka, Malaysia

<sup>b</sup>Faculty of Technology Engineering (FTK), Universiti Teknikal Malaysia Melaka(UTeM), 76100 Durian Tunggal, Melaka, Malaysia

## Article history

Received

22 February 2016

Received in revised form

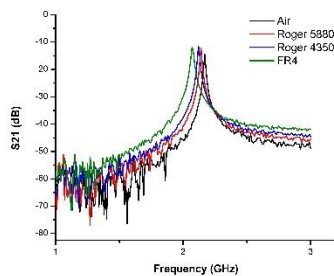
31 May 2016

Accepted

3 August 2016

\*Corresponding author  
zahriladha@utem.edu.my

## Graphical abstract



## Abstract

A new sensor based on symmetrical split ring resonator (SSRR) functioning at microwave frequencies has been proposed in order to detect and characterize the properties of the materials. This sensor is based on perturbation theory, in which the dielectric properties of the material affect the quality factor and resonance frequency of the microwave resonator. Conventionally, coaxial cavity, waveguide, dielectric resonator techniques have been used for characterizing materials. However, these techniques are often large, and expensive to build, which restricts their use in many important applications. Thus, the proposed bio-sensing technique presents advantages such as high measurement sensitivity (around 400 Q-factor) with the capability of suppressing undesired harmonic spurious and permits potentially material characterization and determination. Hence, using a specific experimental methodology, tests performed have demonstrated the biosensor ability to characterize at least four reference materials with known permittivity (Air, Roger Duriod RT 5880, Roger Duriod RT 4530, FR4) and one material with unknown permittivity (Beef). Accordingly, the numerically established relations are experimentally verified for these reference materials and the results indicated that the average estimation error of measuring the permittivity was 2.56 % at resonant of around 2.2 GHz. The proposed design is useful for various applications such as food industry, medicine, pharmacy, bio-sensing and quality control.

Keywords: HFSS, material characterization, microwave biosensor, SSRR

© 2016 Penerbit UTM Press. All rights reserved

## 1.0 INTRODUCTION

Extracting significant information related to the configuration and the quality of the material properties has received a considerable interest over the past few years. The standard permittivity in materials has different molecular structures respond when external RF electric field is applied in different forms. For this reason, the response of any microwave

planar sensor is significantly influenced by the dielectric properties of materials used in the substrate and each tested material demonstrates a unique complex permittivity in the RF and microwave frequency range [1], [2]. The material characterization based on their complex permittivity has applications in various fields such as food industry, quality control, agriculture, bio-sensing, medicine and pharmaceutical industry [3]–[7]. However, the

determination of accurate measurement for complex permittivity of materials is quite challenging task in the field of RF and microwave engineering [8], [9]. Many techniques has been developed for material characterization in various frequency bands which includes transmission-line, free-space [10], [11], near-field sensors [12]–[14], resonant cavity methods [15], [16], and planar resonator techniques [6], [17]–[19].

The resonant cavity methods are generally more accurate for low loss material under test (MUT) compared to other techniques. The conventional waveguide resonant cavity technique is used to characterize the samples of materials under range of microwave frequency band [9], [20]. However, it has the disadvantage of difficulty during the fabrication process due to its kind of cavities. Furthermore, for complex permittivity measurement, the metal waveguide has to be filled with the test material entirely to the volume of the waveguide which leads to significant attenuation of electromagnetic waves. Thus, dimensions of the waveguide have an effect on the sensitivity of complex permittivity measurement.

Recently, the resonant sensors based on planar microstrip has been used to determine and characterize the properties of the materials [19]. This is due to their advantages of having low cost, compact in size, being non-invasive, portability, and ease in sample preparation. However, most of them are suffering from low sensitivity with poor Q-factor which restricts their use in some applications.

Therefore, a high Q-factor resonator sensor based on a symmetrical split ring resonator (SSRR) has been proposed for detecting and determining the properties of the materials. This SSRR has a very narrow bandwidth of the transmitted signals which increase the Q-factor. The standards solids samples with known and unknown permittivity has been tested and measured by using the proposed technique and then compared with existing sensors. Furthermore, the behavior of a symmetrical split ring resonator (SSRR) as a sensor for determining and detecting the properties of the materials is numerically and experimentally analyzed using High Frequency Structural Simulator (HFSS-15). It is believed that the proposed technique is suitable for various industry applications such as food industry, bio-sensing, quality control, agriculture, medicine and pharmaceutical industries.

## 2.0 SENSOR DESIGN AND THEORETICAL ANALYSIS OF PERMITTIVITY EXTRACTION

The configuration and design parameters of SSRR structure are demonstrated in figure 1 (a). Roger corporation® RT/Duroid 5880 was used with substrate thickness of 0.787 mm, loss tangent of 0.0009, and permittivity of 2.20. It has a copper thickness of 17.5  $\mu$ . A cross-sectional dimension of 68 mm x 100 mm, ( $W_g$ ,  $L_g$ ) respectively, is used to model the proposed sensor with a main radius of 15.85 mm ( $r$ ) and 0.37 mm ( $g$ ) gap between the ring and feed-lines. The proposed

sensor is modelled in the High Frequency Structural Simulator (HFSS), and the simulation is carried out to obtain the two-ports scattering parameters in the specified frequency band. The design structure of SSRR has an outer ring of 17.1 mm ( $R_o$ ) and inner ring of 14.6 mm ( $R_i$ ) in the outer ring of SSRR, and an outer ring of 12.1 mm ( $R_1$ ) and inner ring of 9.6 mm ( $R_2$ ) in the inner ring of SSRR. It can be considered to be simple LC circuit with a response frequency  $f_r$ , using the following equation [9], [21].

$$f_r = \frac{1}{2\pi\sqrt{L_r(C_s + C_r)}} \quad (1)$$

Where,  $f_r$  is the SSRR resonant frequency,  $L_r$  and  $C_r$  are the inductance and capacitance associated with SSRR, respectively,  $C_s$  is the capacitance between the ground plane and microstrip-line. The  $C_s$  and  $L_r$  is always considered as constant due to the material under test (MUT) which is usually non-magnetic and a constant permittivity used in the substrate of the proposed sensor.

The resonance frequency change is dependent on interaction between the material under test (MUT) and the electric field of the planar sensor. This interaction makes the MUT perturbs the field distribution which causes a reduction in the resonant frequency as well as reduction in Q-factor. This happens due to the real part and imaginary part of the material permittivity. The variation of resonant frequency is based on the MUT that has different permittivity and properties. The SSRR sensor can detect and characterize the equivalent permittivity and the properties of the materials by analyzing the change of resonant frequency.

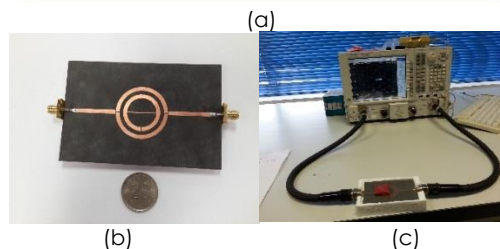
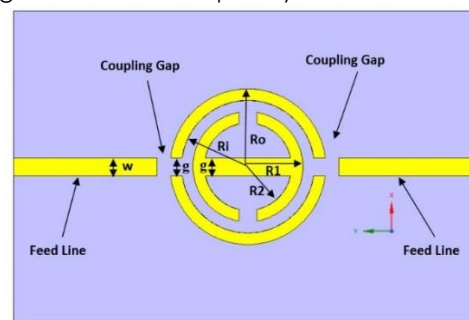


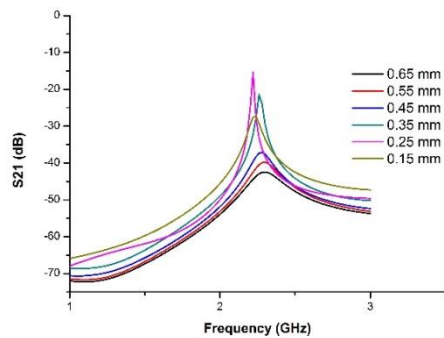
**Figure 1** Schematic of the SSRR sensor (a) Top view of the proposed sensor (Bottom view is considered as ground) (b) Photograph of the fabricated sensor (c) Proposed sensor with MUT connected to VNA.

The proposed sensor is fabricated on the Roger RT/Duroid 5880 substrate as indicated in figure 1 (b). The MUT having a rectangular cross section is placed

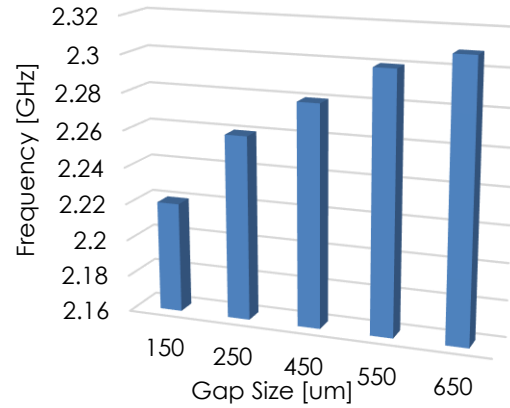
on the maximum electric field region above the resonator sensor as indicated in [19], [22], and the proposed sensor is connected to Agilent Vector Network Analyzer (VNA) through two-ports SMA connectors which shown in figure 1 (c). A calibration using Calibration Kit Agilent was used to calibrate the two-ports of VNA. The solid sample is placed on the top of the sensor which leads to change the resonant frequency. The change of the resonant frequency for each solid sample is recorded which is demonstrated in figure 5. The permittivity of the sample is then extracted from all the tested materials using the derived numerical model (2) by means of the measured frequency.

### 3.0 RESULTS AND DISCUSSION

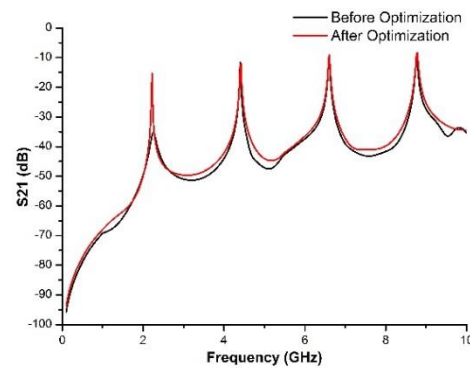
From figure 2 (c), it can be observed that the Q-factor in the SSRR sensor has low value at 2.26 GHz operating frequency compared to the other harmonic resonant frequencies before the optimization was made. Due to the fact of the effect of coupling loss (gap between the ring and the feed lines), an optimization was done in order to produce a maximum field distribution of the operating frequency and provides minimum insertion loss and resonating frequency shift [Figure 2 (b)]. A comparison before and after optimization of the proposed sensor is indicated in table 1. It demonstrates that the SSRR sensor has achieved a high Q-factor around 407.34 at the operating frequency with the less insertion loss after optimization was made. This is due to the fact that the gap has a significant effect on determination of the dielectric properties. Another reason is that the field of microstrip ring resonator is noticeably disturbed with a small coupling gap while in larger coupling gap size, it has less disturbance with high losses in the coupling gap region. Thus, the variations of the coupling gaps were evaluated using a gap size of 0.15 to 0.35 mm as indicated in figure 2 (a).



(a)



(b)



(c)

**Figure 2** (a) An optimization of the coupling gap effects (b) Effects of the coupling gap in resonant frequency shift (c) Transmission coefficient result before and after optimization

**Table 1** Comparison before and after optimization process

| Mode (n) | Before Optimization |          |          | After Optimization |          |          |
|----------|---------------------|----------|----------|--------------------|----------|----------|
|          | Freq (GHz)          | Q-Factor | S21 (dB) | Freq (GHz)         | Q-Factor | S21 (dB) |
| 1        | 2.26                | 33.98    | -35.19   | 2.22               | 407.34   | -15.32   |
| 2        | 4.40                | 517.65   | -11.61   | 4.42               | 243.53   | -12.03   |
| 3        | 6.60                | 379.31   | -10.09   | 6.60               | 368.72   | -8.99    |
| 4        | 8.76                | 369.62   | -9.66    | 8.76               | 302.07   | -8.64    |

The simulation and measurement of transmission coefficient results are demonstrated in figure 3. The obtained operating frequency from the simulation is found in a very good agreement with the measurement result. It obviously illustrates that the proposed sensor has narrower band and sharper dip which reveals its high Q nature compared to other structures. Furthermore, the results demonstrate some small deviations between the simulation and measurement. Therefore, the measured resonance frequencies are slightly shifted from the simulation and the insertion loss magnitude is lower than simulated one. The reason behind this is because of the mismatch between the feed-lines and SMA

connectors, and also the tolerance of fabrications which limits in simulation accuracy.

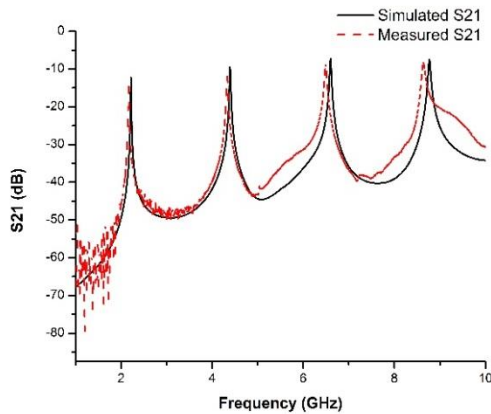


**Figure 3** Simulated and measured S21 transmission coefficients in dB

Table 2 summarizes a comparison of the simulated and measured responses between the existing sensor and the proposed SSRR sensor. From the results, it can be concluded that proposed sensor has higher Q-factor with low insertion loss compared to other sensors in [23].

**Table 2** Comparison between the proposed SSRR sensor and others in term of resonance frequency, Q-factor and transmission magnitude S21 in dB

| Sensor Type       | Simulation |          | Q-Factor or | Measurement |          |
|-------------------|------------|----------|-------------|-------------|----------|
|                   | Freq (GHz) | S21 (dB) |             | Freq (GHz)  | S21 (dB) |
| Aligned-Gap [23]  | 5          | -25.60   | 240         | 4.90        | -16.79   |
| Centered-Gap [23] | 4.98       | -23.30   | 150         | 4.53        | -15.26   |
| Proposed SSRR     | 2.22       | -15.32   | 407         | 2.20        | -14.45   |

A various dielectric samples from 1 to 10 were loaded and simulated in the proposed SSRR sensor in order to visualize the design of sensing applications. Figure 4 demonstrates the resonance frequency which is shifted down accordingly when the value of the dielectric constant of the sample is increased. The reason why the frequency shifts down is because of the high capacitance particularly when placing the dielectric material which basically interacts with the electric field of the sensor. Moreover, this can be proved by Equation (1), which is increasing the capacitance that will produce a low resonance frequency. The shifts of resonance frequency are considered as data which are related to the permittivity of the MUT ( $\epsilon$ ). Thus, an expression for the relationship between the permittivity,  $\epsilon$  and frequency,  $f$  of the MUT is required. This expression can

be modeled by using curve fitting method based on the data presented in figure 4 and the polynomial presented in the figure is obtained as follows:

$$\epsilon = 85.06 f^2 - 425.69 f + 525.57 \quad (2)$$

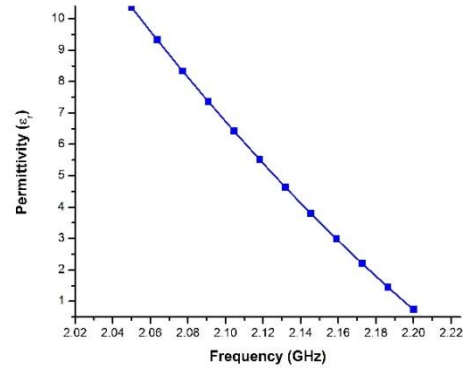


**Figure 4** MUT permittivity as a function of resonance frequency for the proposed SSRR sensor

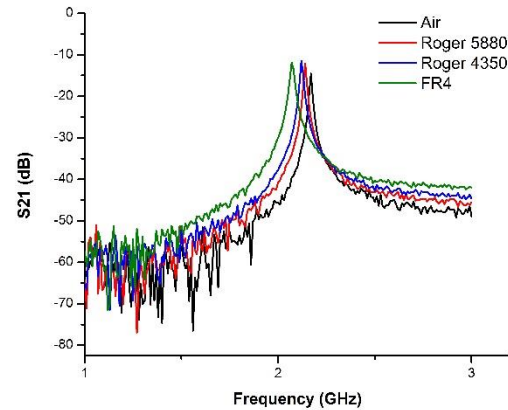


**Figure 5** Changes in resonance frequency when known permittivity of MUT is tested

Various samples were used in order to validate the proposed SSRR sensor and estimate their potential of dielectric detecting and sensing. These samples are FR4, Duriod RT 5880, Air, and Duriod RT 4530 and they were placed on the maximum E-field area of the sensor. The electric field interacts with these samples which caused shifting in the resonant frequency. For the conducted experiment, the resonance frequency is shifted to lower frequency and it is directly proportional to the permittivity of the dielectric MUT.

Four MUT such as Air, Duriod RT 5880, Duriod RT 4530 and FR4 were used as calibration samples since their dielectric constant is well known, in order to observe the changes in resonant frequency and the relation to the permittivity of materials. Thus, the materials with unknown permittivity can be extracted. Figure 5 demonstrates the changes of resonant frequency for

the materials with known dielectric constant. The experimental results and the extracted permittivity value of each material under test (MUT) are summarized in Table 3.

**Table 3** summary of experimental results for the proposed SSRR sensor

| MUT            | Reference Permittivity | Calculated Permittivity |
|----------------|------------------------|-------------------------|
| Air            | 1                      | 0.94                    |
| Duriod RT 5880 | 2.2                    | 2.12                    |
| Duriod RT 4350 | 3.48                   | 3.5                     |
| FR4            | 4.4                    | 4.45                    |
| Beef           | 56.5                   | 55.98                   |

## 4.0 CONCLUSION

This paper presents a new symmetrical split ring resonator based metamaterials for dielectric sensing purposes. This sensor provides greater sensitivity by introducing a sharper and narrower bandwidth which contributes to a high Q-factor by comparing it to the conventional designs of SSRs. The obtained resonant frequency from the simulation is found in a very good agreement with the measurement result. The frequency is shifted to lower frequency accordingly while the value of the permittivity is increased. The shift is based on transmission coefficients S<sub>21</sub> (dB) which is considered as a function of permittivity of MUT. Known permittivity of materials were used and tested in order to verify the sensor's sensitivity. It has been demonstrated through conducted experiment activities, that the proposed SSRR resonator is the promising candidates to be adopted as sensor in many sensing applications such as bio-sensing, food industry, quality control, agriculture, medicine and pharmaceutical industries.

## Acknowledgement

This work was supported by UTeM Zamalah Scheme and funded by UTeM and the Malaysian Government (MOHE) for research grant RAGS/1/2014/TK03/UTEM/FTK-B00078. The authors would like to thank TMAC Malaysia.

## References

- [1] Von, A. R. and Hippe. 1954. *Dielectric Materials and Applications*. John Wiley and Sons. 77: 284-438
- [2] Kulkarni, S. and M. S. Joshi. 2015. Design and Analysis of Shielded Vertically Stacked Ring Resonator as Complex Permittivity Sensor for Petroleum Oils. *IEEE Transactions on Microwave Theory and Techniques*. 63(8): 2411–2417.
- [3] Shaji, M. and M. J. Akhtar. 2013. Microwave Coplanar Sensor System for Detecting Contamination in Food Products. *IEEE MTT-S International Microwave and RF Conference*. 14-16 December 2013. 1–4.
- [4] Jha, A. K. and M. Jaleel Akhtar. 2013. Automated RF Measurement System for Detecting Adulteration in Edible Fluids. *IEEE Applied Electromagnetics Conference (AEMC)*. 18-20 December 2013. 1–2.
- [5] Celik, N., R. Gagari, G. C. Huang, M. F. Iskander, and B. W. Berg. 2014. Microwave Stethoscope: Development and Benchmarking of a Vital Signs Sensor Using Computer-Controlled Phantoms and Human Studies. *IEEE Transactions on Biomedical Engineering*. 61(8): 2341–2349.
- [6] Boybay, M. S. and O. M. Ramahi. 2013. Non-Destructive Thickness Measurement Using Quasi-Static Resonators. *IEEE Microwave and Wireless Components Letters*. 23(4): 217–219.
- [7] Wee, F. H., P. J. Soh, a. H. Suhaizal, H. Nornikman, and a. a. Ezanuddin. 2009. Free Space Measurement Technique on Dielectric Properties of Agricultural Residues at Microwave Frequencies. *SBMO/IEEE MTT-S International Microwave and Optoelectronics Conference (IMOC)*. 3-6 November 2009. 183–187.
- [8] Ansari, M. A. H., A. K. Jha, and M. J. Akhtar. 2015. Design and Application of the CSRR-Based Planar Sensor for Noninvasive Measurement of Complex Permittivity. *IEEE Sensors Journal*. 15(12): 7181–7189.
- [9] Ansari, M. A. H., A. K. Jha, and M. J. Akhtar. 2015. Permittivity Measurement of Common Solvents Using the CSRR Based Sensor. *IEEE International Symposium on Antennas and Propagation & USNC/URSI National Radio Science Meeting*. 19-24 July 2015. 1199–1200.
- [10] Ghodgaonkar, D. K., V. V. Varadan, and V. K. Varadan. 1990. Free-space Measurement of Complex Permittivity and Complex Permeability of Magnetic Materials at Microwave Frequencies. *IEEE Transactions on Instrumentation and Measurement*. 39(2): 387–394.
- [11] Kadaba, P. K., 1984. Simultaneous Measurement of Complex Permittivity and Permeability in the Millimeter Region by a Frequency-Domain Technique. *IEEE Transactions on Instrumentation and Measurement*. IM-33(4): 336–340.
- [12] Stuchly, M. A. and S. S. Stuchly. 1980. Coaxial Line Reflection Methods for Measuring Dielectric Properties of Biological Substances at Radio and Microwave Frequencies-A Review. *IEEE Transactions on Instrumentation and Measurement*. IM-29(3): 176–183.
- [13] Ganchev, S. I. and N. Qaddoumi. 1995. Calibration and Measurement of Dielectric Properties of Finite Thickness Composite Sheets with Open-Ended Coaxial Sensors. *IEEE Transactions on Instrumentation and Measurement*. 44(6): 1023-1029.
- [14] Misra, D., M. Chhabra, B. R. Epstein, M. Mirotznik, and K. R. Foster. 1990. Noninvasive Electrical Characterization of Materials at Microwave Frequencies Using an Open-Ended Coaxial Line: Test of an Improved Calibration Technique. *IEEE Transactions on Microwave Theory and Techniques*. 38(1): 8–14.
- [15] Teodoridis, V., T. Spicopoulos, and F. E. Gardiol. 1985. The Reflection from an Open-Ended Rectangular Waveguide Terminated by a Layered Dielectric Medium. *IEEE Transactions on Microwave Theory and Techniques*. MTT-33(5): 359-366.
- [16] Ghasr, M. T., D. Simms, and R. Zoughi. 2009. Multimodal Solution for a Wiveguide Radiating Into Multilayered Structures-Dielectric Property and Thickness Evaluation. *IEEE Transactions on Instrumentation and Measurement*. 58(5): 1505–1513.
- [17] Lee, C. S., and C. L. Yang. 2014. Thickness and Permittivity Measurement in Multi-Layered Dielectric Structures Using Complementary Split-Ring Resonators. *IEEE Sensors Journal*. 14(3): 695–700.
- [18] Kang, B., J. Cho, C. Cheon, and Y. Kwon. 2005. Nondestructive Measurement of Complex Permittivity and Permeability Using Multilayered Coplanar Waveguide Structures. *IEEE Microwave and Wireless Components Letters*. 15(5): 381–383.
- [19] Alahnomi, R. A., Z. Zakaria, E. Ruslan, and A. A. M. Isa. 2015. Optimization Analysis of Microwave Ring Resonator for Bio-

- sensing Application. *International Journal of Applied Engineering Research*. 10(7): 18395–18406.
- [20] Jha, A. K. and M. J. Akhtar. 2014. A Generalized Rectangular Cavity Approach for Determination of Complex Permittivity of Materials. *IEEE Transactions on Instrumentation and Measurement*. 63(11): 2632–2641.
- [21] Zhou, X. H. J., P. Jia, Y. Zhang. 2013. High sensitive biosensor based on aSRR and High-Impedance Microstrip Line. *2nd International Conference on Measurement, Information and Control*. 16-18 August 2013. 234–237.
- [22] Alahnomi, R. A., Z. Zakaria, E. Ruslan, and A. A. M. Bahar. 2016. A Novel Symmetrical Split Ring Resonator Based on Microstrip for Microwave Sensors. *Measurement Science Review*. 16(1): 21-27.
- [23] Rusni, I. M., A. Ismail, A. R. H. Alhawari, M. N. Hamidon, and N. A. Yusof. 2014. An Aligned-Gap and Centered-Gap Rectangular Multiple Split Ring Resonator for Dielectric Sensing Applications. *Sensors*. 14(7): 13134–48.